Pathway-specific light adaptation in human electroretinograms

Alódia Brasil

Biological Sciences Institute, Federal University of Para, Belém, Brazil
Department of Ophthalmology, University Hospital Erlangen, Erlangen, Germany

Tina I. Tsai

Department of Ophthalmology, University Hospital Erlangen, Erlangen, Germany

Givago da Silva Souza

Biological Sciences Institute, Federal University of Para, Belém, Brazil
Tropical Medicine Nucleus, Federal University of Para, Belém, Brazil ✉

Anderson Manoel Herculano

Biological Sciences Institute, Federal University of Para, Belém, Brazil

Dora Fix Ventura

Institute of Psychology, University of São Paulo, São Paulo, Brazil ✉

Luiz Carlos de Lima Silveira*

Biological Sciences Institute, Federal University of Para, Belém, Brazil
Tropical Medicine Nucleus, Federal University of Para, Belém, Brazil
Ceuma University, Sao Luis, Brazil

Jan Kremers

Department of Ophthalmology, University Hospital Erlangen, Erlangen, Germany 🏠 ✉

The cellular origins of slow ERG changes during light adaptation following a dark-adapted state are still unclear. To study light adaptation, six healthy, normal trichromats were dark-adapted for 30 min prior to full-field ERG recordings to sinusoidal stimuli that isolate responses of the L- or M-cones or that stimulate luminance and chromatic mechanisms at 12 or 36 Hz. Recordings were performed for 16 min with 2-min intervals after onset of a constant background. Generally, the responses were sine-wave-like, and the first harmonic (fundamental) component dominated the Fourier spectrum except for the 12-Hz luminance stimulus in which two components, a sine-wave-like component and a transient component, determined the response profiles, leading to large second harmonic components. The amplitude of the first harmonic component (F) increased as a function of the light-adaptation time except for the 12-Hz luminance stimulus at which the F component decreased as a function of the light-adaptation period. The phase of the first harmonic component changed only slightly (less than 30°) during the light-adaptation period for all stimuli conditions. The L/M ratio in luminance reflecting ERGs decreased with increasing adaptation time. Our present data suggest that the light-adaptation process mainly reflects changes in the luminance pathway. The responses to 12-Hz luminance stimuli are determined by two different luminance driven pathways with different adaptation characteristics.

Introduction

The electroretinogram (ERG) is a noninvasive electrophysiological method widely used in the clinic to evaluate retinal function. It is used to detect, diagnose, and monitor disease-related functional alterations in the retina. Recently, the ERG has obtained importance in basic research because it has been shown that the ERG can be used to study normal physiological processes within different retino-geniculate pathways (Jacob et al., 2015; Kremers & Link, 2008; Kremers, Rodrigues, de Lima Silveira, & da Silva Filho, 2010; Martins et al., 2016; Parry et al., 2012).

The ERG was found to change during light adaptation following an extended period in the dark (Armington & Biersdorf, 1958; Burian, 1954). For the standard full-field ERG response to a single high-intensity flash, the cone-driven a-wave, b-wave, i-wave, and oscillatory potentials gradually increase in amplitude during light adaptation. The ERG amplitude change is accompanied by a concomitant decrease in the components' implicit time (Alexander, Raghuram, & Rajagopalan, 2006; Armington & Biersdorf, 1958; Benoit & Lachapelle, 1995; Burian, 1954; Gouras & MacKay, 1989; Murayama & Sieving, 1992; Peachey, Alexander, Fishman, & Derlacki, 1989). These changes in amplitude and implicit times are slow, and the time courses of adaptation are in the order of several minutes. Flicker ERGs elicited by trains of flashes or sine-wave modulation at high temporal frequencies show a similar light adaptation. The ERG amplitudes increase and phases decrease within the first 5 min of exposure to the adapting field, after which the changes slow down until a plateau is reached after around 10 min (McAnany & Nolan, 2014; Peachey, Alexander, Derlacki, & Fishman, 1992; Peachey, Alexander, & Fishman, 1991). Hence, the International Society for Clinical Electrophysiology of Vision recommends adapting the eye to a light background for at least 10 min after being completely dark adapted before making photopic ERG measurements (McCulloch et al., 2015).

Understanding and establishing the changes that underlie light adaptation in normal visual systems also has clinical relevance. For example, patients with incomplete congenital stationary night blindness and with retinitis pigmentosa can show different amplitude changes during light adaptation to 30-Hz flicker stimuli in comparison with healthy subjects (Miller & Sandberg, 1991; Miyake, Horiguchi, Ota, & Shiroyama, 1987). Thus, the kinetics of light adaptation may shed light on the pathophysiological mechanisms and may be used as a functional biomarker for the mentioned diseases.

Several hypotheses regarding the underlying mechanisms of photopic ERG changes during light adaptation have been proposed (Armington & Biersdorf, 1958; Cameron & Lucas, 2009; Gouras & MacKay, 1989; Kondo et al., 1999; Matthews, Murphy, Fain, & Lamb, 1988; Normann & Perlman, 1979), two of which are still in play. One proposes that the phenomenon is caused by a slow re-depolarization of cone photoreceptors (after initial hyperpolarization) during light adaptation (Burkhardt & Gottesman, 1987; Dowling & Ripps, 1971; Gouras & MacKay, 1989). The time course of ERG and cone membrane potential alterations after the onset of an adapting light resemble each other (Matthews et al., 1988; Normann & Perlman, 1979). The second hypothesis involves the gradual decrease of a suppressive effect from rod phototransduction on cone-driven ERG responses (Arden & Frumkes, 1986). This view was reinforced by Kondo et al. (1999) by revealing greater amplitude increases during light adaptation in the rod-dominated retinal periphery. Further support comes from work with $Gnat1^{-/-}$ mice. These mice are devoid of the α-subunit of rod transducin and, thus, do not have functional rods. The amplitude growth and the decrease in implicit time of the photopic b-wave during light adaptation were smaller in these mice compared to wild-type animals (Cameron & Lucas, 2009).

Recently, in an attempt to further describe the nature and extent of the flicker ERG response changes, McAnany and Nolan (2014) took a different approach. They measured the responses to 31.25-Hz sine-wave luminance modulation and extracted the first (fundamental, F), second (2F), and third (3F) harmonic components using Fourier transform. These parameters were then modeled with the inverse of an exponential function to obtain an estimate of the time constants and magnitudes of change in ERG amplitudes and phases to evaluate their kinetics. Interestingly, they showed that from 0 to 15 min of light adaptation, the different harmonic components show distinct changes: The amplitudes and the time constants of harmonic components changed differently. The F phase did not change with adaptation time, whereas the phases of the 2F and 3F components increased by approximately 45° with a time constant of about 2 min. This finding brings into question whether a general mechanism underlies all ERG response changes or whether they differ between signals originating in different cone photoreceptor types or postreceptoral pathways. If the changes depend on only one general mechanism, then it can be expected that their dynamics are the same for all retinal circuitries. On the other hand, if the different pathways have distinct adaptation mechanisms, then the dynamics of the changes may depend on the stimulated circuitry. This fact would also mean that the theories proposed to date might only be partly correct.

The present study aims to investigate how different retinal mechanisms change their activity during the

light-adaptation period. Specifically, the characteristics and dynamics of the signals originating in the L- and M-cone–driven subsystems were separately assayed using the triple silent substitution technique (Estévez & Spekreijse, 1982; Estévez & Spekreuse, 1974; Kremers, 2003). Moreover, the red–green chromatic and the luminance mechanisms were studied using counterphase and in-phase modulation of the outputs of the red and green light-emitting diode (LED) sources, respectively (Kremers et al., 2010). The ERGs were recorded at two separate temporal frequencies known to favor the luminance, magnocellular (30 Hz) and the L-M opponent, parvocellular (12 Hz) retino-geniculate pathways (Jacob et al., 2015; Kremers & Link, 2008; Kremers & Pangeni, 2012; Kremers et al., 2010; Martins et al., 2016; Parry et al., 2012).

Methods

Subjects

Six healthy subjects (two males, four females, ages between 26 and 35 years) with no history of eye disease or color vision defects (HMC anomaloscope color vision test, Oculus Optikgeräte GmbH, Wetzlar, Germany) participated in the experiments. All subjects signed an informed consent and underwent ophthalmological evaluations on the first day of measurements. The experiments adhered to the tenets of the Declaration of Helsinki and were approved by the ethics committee of the medical faculty of the University of Erlangen-Nürnberg.

Visual stimuli

Measurements were carried out using the RETIport recording system (Roland Consult, Wiesbaden, Germany). The stimuli were sine waves presented using a six-primary Ganzfeld bowl (Q450 SC; Roland Consult). The primaries consisted of arrays of LEDs, of which only four were used in the following protocols: green (peak wavelength 523 nm, CIE1931 coordinates: $x = 0.2016$, $y = 0.7371$), orange (594 nm, CIE1931 coordinates: $x = 0.5753$, $y = 0.4240$), blue (469 nm, CIE1931 coordinates: $x = 0.1255$, $y = 0.0926$), and red (638 nm, CIE1931 coordinates: $x = 0.6957$, $y = 0.2966$). All responses were recorded under identical mean luminance (284 cd/m^2; the luminance of each LED array: green 40 cd/m^2, orange 160 cd/m^2, blue 4 cd/m^2, and red 80 cd/m^2) and chromaticity (i.e., reddish appearance, CIE1931 coordinates: $x = 0.5951$, $y = 0.3857$). The luminance measurements were made using a Minolta LS-110 photometer. Spectral outputs and

| | Stimulus | | | |
LED	L-cone	M-cone	Isochromatic luminance	Isoluminant chromatic
Mean luminance (cd/m^2)	284	284	284	284
Luminance (cd/m^2)				
Green	40	40	40	40
Orange	160	160	160	160
Blue	4	4	4	4
Red	80	80	80	80
LED contrast, %				
Green	5.0	−20	75	−100
Orange	−22	59	75	0
Blue	−1	0	75	0
Red	90	−90	75	50
Cone contrast, %				
L	19	0	75	6.5
M	0	18	75	−18.5
S	0	0	75	−9.0
Rod	0	0	75	−48.3
Frequency, Hz	12	12	12	12
	36	36	36	36

Table 1. Stimulus conditions. *Note*: Contrasts with opposite signs indicate counterphase modulation.

CIE coordinates were measured using a CAS 140 spectroradiometer (Instrument Systems, Munich, Germany).

Eight stimulus protocols were employed in total: L-cone isolating, M-cone isolating, isochromatic luminance, and isoluminant red–green chromatic stimuli, each at 12 and 36 Hz temporal frequencies. Stimulus specifications of each of these are presented in Table 1.

Briefly, L- or M-cone isolation was obtained using the triple silent substitution method (Kremers, 2003; Shapiro, Pokorny, & Smith, 1996). L-cone responses were isolated with 19% cone contrast with all other photoreceptor types silenced (i.e., 0% modulation). Similarly, M-cone isolation was obtained with 18% cone contrast and with L-cone, S-cone, and rods silenced. These stimuli were presented at 12 and 36 Hz to assess separate contributions from the chromatic- and luminance-based pathways, respectively (Jacob et al., 2015; Kremers & Link, 2008; Kremers & Pangeni, 2012; Kremers et al., 2010; Martins et al., 2016; Parry et al., 2012). Additional measurements with isochromatic luminance and isoluminant red–green chromatic stimuli were performed at 12 and 36 Hz. For the luminance stimuli, the outputs of all four LEDs were modulated in phase with 75% luminance contrast. The red–green chromatic stimuli were obtained with counterphase modulation of the red and green LEDs (blue and orange LEDs not modulated). Modulation contrast was 100% for the green and 50% in the red LEDs to

achieve isoluminance considering that the mean luminance of the red LED (80 cd/m^2) was twice that of the green LED (40 cd/m^2). Due to individual variation in isoluminance conditions, residual luminance stimulation may be present. However, previous data have shown that, with these conditions, the ERG response to the chromatic contents of the stimulus dominates at 12 Hz (Kremers et al., 2010).

ERG recordings

ERGs were measured from the right eye of each subject. The left eyes were covered by a patch. After dilation with a drop of 0.5% tropicamide, gold cup electrodes filled with electrode paste (DO Weaver & Company) were secured to the forehead and ipsilateral temple as ground and reference electrodes, respectively. The skin areas were cleaned with Nuprep abrasive skin preparing gel (DO Weaver & Company). The active electrode was a corneal fiber electrode placed over the lower conjunctiva, attached at the inner and outer canthus. Corneal anesthesia was not required for any of the subjects. Electrode impedances were kept below 5 kΩ.

Before each of the eight protocols, the subjects were dark-adapted for 30 min in the experimental room with all light extinguished. During this period, both eyes were additionally covered with black eye patches. Directly after, only the right eye was uncovered to be tested, and the subjects were asked to fixate on a small red central point. Their heads were stabilized by forehead and chin rests in front of the Ganzfeld device.

Recordings began 30 s after the adapting field was switched on (i.e., 30 s post light onset = time 0). This time was needed to minimize squint and blink artifacts due to visual discomfort from the sudden photopic condition. Measurements were repeated every 2 min until 16 min lapsed (i.e., at nine time points) under a light steady background. An average measurement consisted of 40 sweeps, each sweep lasting 1 s. One protocol (including the first 30 min dark adaptation) took approximately 47 min to complete. Thus, several recording sessions (of up to four adaptation cycles per session) were required for each subject.

Analysis

ERG responses were Fourier analyzed using a self-written MATLAB program (version R2011b; MathWorks, Natick, MA) to obtain amplitudes and phases of the first harmonic (F) component. For luminance 12 Hz, we also considered the amplitudes of the second harmonic component (2F) because it was previously found that, in this condition, 2F is larger than F

(Pangeni, Horn, & Kremers, 2010). The present study confirms this finding (see Results section). The signal-to-noise ratio (SNR) was defined as the amplitudes at the analysis frequency [Amp (F)] divided by the average of the amplitudes at the adjacent frequencies, [Amp(F ± 1 Hz)] (Meigen & Bach, 1999):

$$SNR = \frac{2 \times Amp(F)}{Amp(F-1) + Amp(F+1)}. \quad (1)$$

Similarly the SNR for 2F at the 12-Hz luminance condition was considered. The SNR was used as criterion to exclude data points of the analysis as described later in this section.

For each stimulus condition, we calculated the relative amplitude (i.e., the ratio between the amplitude in each time point and the amplitude obtained at time 0) and the phase change of the ERGs relative to the first measurement. We considered three criteria for excluding data: (a) phase data were not used if the SNR was less than two (Meigen & Bach, 1999). Meigen and Bach (1999) actually recommended an SNR of 2.89, but they only considered response amplitudes and not phases. We found that the response phases were still in the expected range (defined as phases that did not differ from those obtained at other adaptation times by more than 25°) for SNRs larger than two, indicating that these responses were reliable. For SNRs that were only slightly less than two, phases could be used if they were in the same range of phases obtained at other time points at which the SNR was larger than two. (b) All phase data from a condition and a subject were excluded from the analysis when the SNR at $t = 0$ min was less than two, and the phases did not fit in the curve. (c) A nonparametric Friedman test was performed to test whether amplitude and phase differences after 16 min of adaptation in comparison with directly after adaptation onset were significant (SPS version 21.0). Parameters a and τ were compared separately. We considered significance when $p < 0.05$. The level of significance was divided by the number of tests to correct for multiple testing (8 stimulus conditions × 2 outcomes [amplitudes and phases] = 16 plus amplitudes of the second harmonic for the 12-Hz luminance condition). As a result, significance was reached for $p < 0.003$ (= 0.05/17). Only data in which a significant change was found were considered for further evaluation. The averaged relative ERG data were fitted by Equation 2 (Alexander et al., 2006; McAnany & Nolan, 2014):

$$y(t) = y(0) + a \times \left(1 - \exp\left(\frac{-t}{\tau}\right)\right) \quad (2)$$

in which $y(t)$ is the response amplitude or phase at time t, $y(0)$ is the amplitude or phase at the first measurement (30 s) after onset of the adapting light, a represents the total change in relative amplitude or
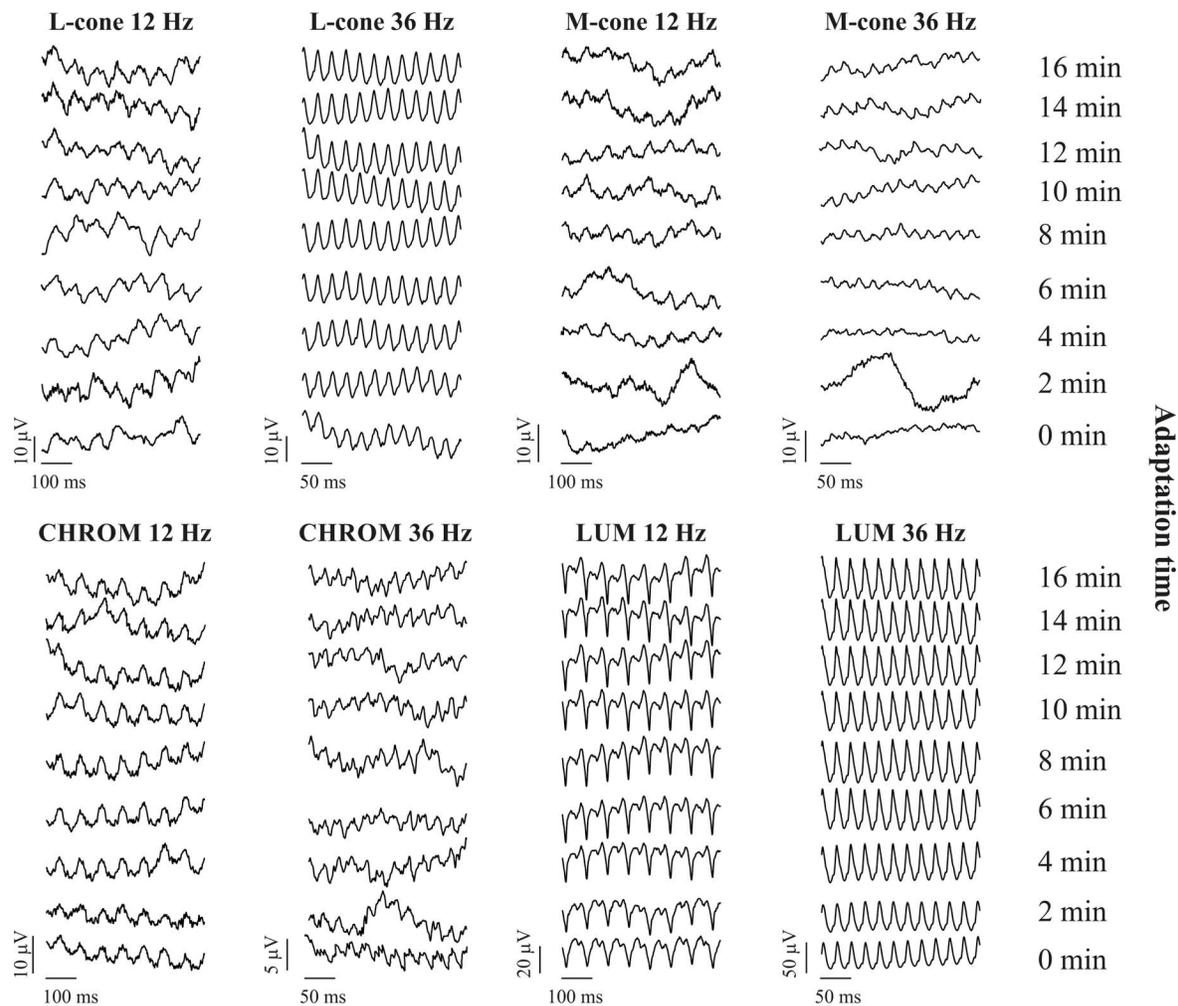
Figure 1. Group-averaged ERG traces for each stimulus condition during 16 min of light adaptation. Time points of each measurement are given on the far right. L-cone = L-cone isolating stimulus; M-cone = M-cone isolating stimulus; CHROM = chromatic stimulus; LUM = luminance stimulus.

phase, and τ is the time constant and was considered as an indicator for speed of light adaptation for each mechanism. This model was fitted to the ERG data using a self-written MATLAB program to obtain estimates of $y(0)$, a, and τ.

Results

ERG waveforms and power spectrum

Group-averaged ERG traces measured at the nine time points after adaptation light onset are shown for each stimulus condition in Figure 1. Particularly, the 36-Hz responses grew over time after start of the light adaptation. The responses to some stimulus conditions (e.g., M-cone isolating stimuli at 36 Hz) were small at $t = 0$ min. For other conditions, the SNR was

satisfactory at $t = 0$ min. In general, most of the stimulus conditions elicited simple sinusoidal-like waveforms that did not change over adaptation time. One exception was the ERG response to the 12-Hz luminance modulation (Figure 1, lower row, third from the left) in which a complex waveform with two maxima and two minima per period was found. This is also the only stimulus condition at which the ERG waveform changed distinctly over time and became more complex. We previously proposed that the ERG responses to 12-Hz sine-wave luminance stimuli contain two (one "sine-like" and one "transient") components (Pangeni et al., 2010). These components could also be detected in the present study with 12-Hz luminance stimuli, resulting in a frequency-doubled response. The waveforms in the present study indicate that these components change with different time courses during light adaptation with the transient response relatively large directly after onset of the adaptation light. In the course of light adaptation, the
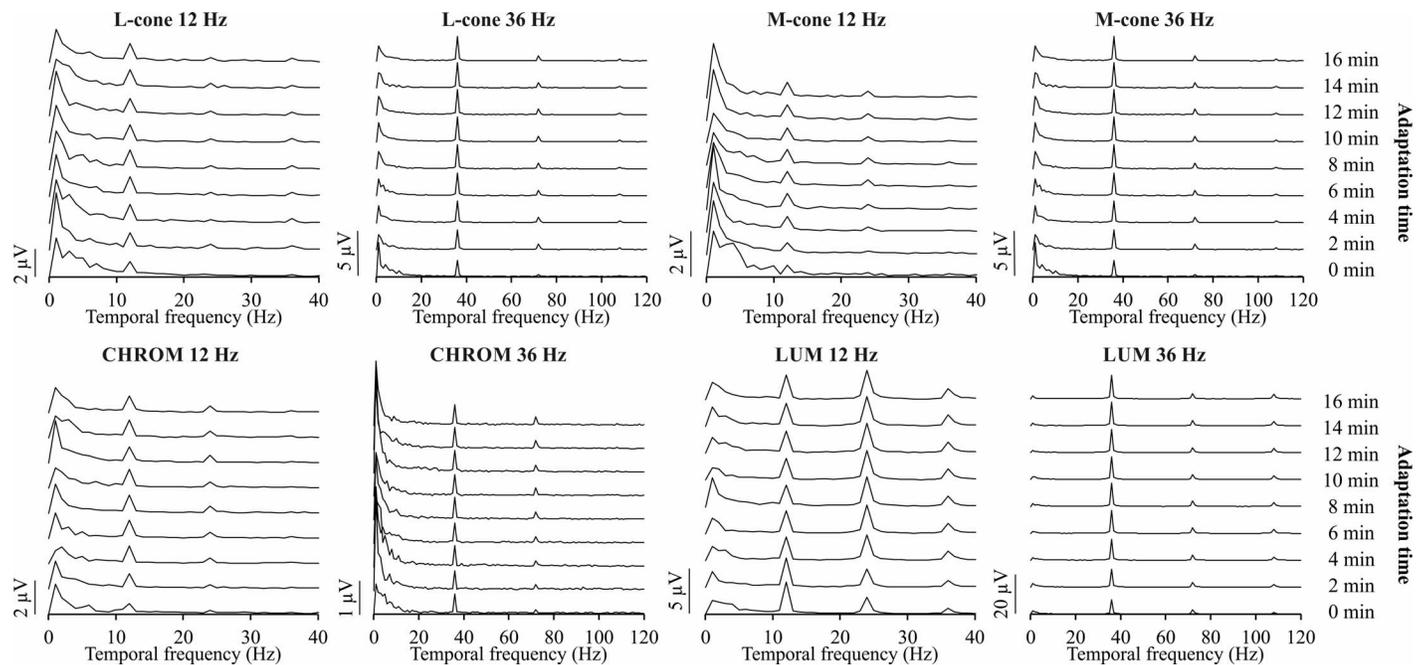
Figure 2. The amplitude as a function of temporal frequency of the group-averaged ERG responses for the eight stimulation conditions plotted separately for the different time points after light onset (given at far right). L-cone = L-cone isolating stimulus; M-cone = M-cone isolating stimulus; CHROM = chromatic stimulus; LUM = luminance stimulus.

sine-wave-like component became relatively larger. As a result, the responses were more complex after 16 min of adaptation.

The amplitude spectra of the group-averaged ERG responses (Figure 2) reveal how the amplitudes in the frequency domain change over time. All responses except those to the 12-Hz luminance stimuli were dominated by the F component. In some conditions, the F component increased during light adaptation. For the 12-Hz luminance responses, F was larger than 2F at $t = 0$ and 2 min, whereas it was reversed at the other time points because the amplitude of F decreased over time while the 2F amplitude increased. This reflects the abovementioned waveform changes observed for this condition.

ERG amplitude and phase as a function of light-adaptation duration

Figure 3 shows the mean ($\pm SD$) response amplitudes of F normalized to the amplitude at $t = 0$ as a function of the adaptation time for all eight conditions. Figure 4 shows the mean ($\pm SD$) phase changes of F plotted versus adaptation time for all eight conditions. Equation 2 was fitted to the mean data. Furthermore, the results of the statistical analyses are shown, indicating if the changes were significant or not. The estimated values of a and τ are displayed for those for which the changes were significant (nonparametric

Friedman test of the difference between the amplitude and phase values obtained after 16 min of adaptation in comparison with directly after adaptation onset). Because the statistics were corrected for multiple testing, some changes that appeared to be systematic did not reach statistical significance. In general, the response amplitudes and phases mainly changed for 36-Hz stimuli containing a substantial luminance modulation (i.e., luminance and L- and M-cone isolating stimuli). Figure 5 shows the normalized amplitudes and phase changes for 2F in the luminance 12-Hz condition. Again, the changes were significant. We previously found that the responses to 12-Hz L- and M-cone isolating are mainly reflecting activity of the red–green chromatic channel (Kremers & Link, 2008; Kremers et al., 2010; Parry et al., 2012).

Relative change (a) and time constants (τ)

For those conditions in which the amplitudes and phases changed significantly, the estimates of a (the change in relative amplitude or phase during the light-adaptation period) and time constants τ are shown in the insets of the graphs. All estimates of a obtained from the amplitude data were positive, indicating an increase in relative response amplitudes. Furthermore, the relative amplitude changes varied between about 0.5 (50%) and 2 (200%). Observe that the F amplitude increases for the 36-Hz luminance and L-cone isolating
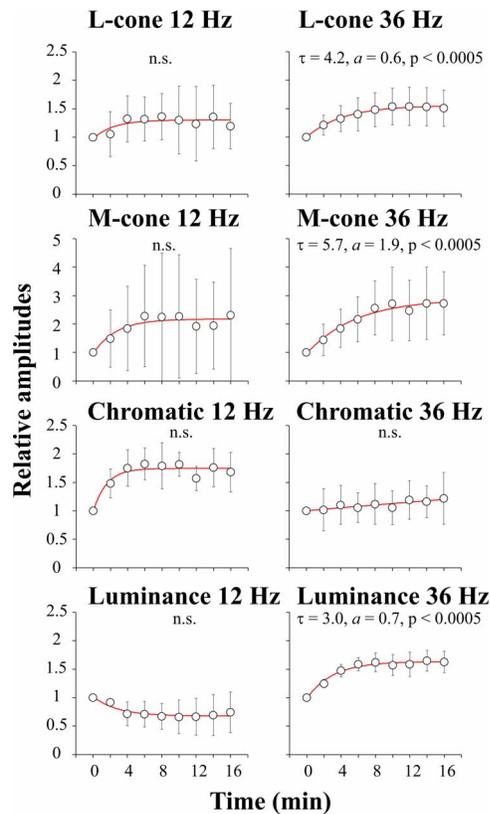
Figure 3. Averaged ($\pm SD$) normalized amplitude changes of the fundamental component (F) normalized to the amplitude at $t = 0$ as a function of adaptation time for the eight different stimulus conditions. The curves are fits of the data with Equation 2. P values are given for significant changes. Not significant = n.s. The estimates of a and τ are displayed for the conditions with significant changes.

Figure 4. Averaged ($\pm SD$) phase shifts of the fundamental component (F) compared to the phase at $t = 0$ as a function of adaptation time for the eight different stimulus conditions. The data are presented in a similar manner as in Figure 3.

stimuli are about 0.6, whereas the increase in the M-cone isolating conditions is about 1.9, i.e., more than a factor of three larger, indicating a decrease in L/M ratio with adaptation time as is discussed in more detail below.

One exception is the F component in the luminance 12-Hz stimulus although this change did not reach significance level. This probably reflects the above-mentioned increase in complexity and the dominance of 2F (Burns, Elsner, & Kreitz, 1992; Kondo & Sieving, 2001; Odom, Reits, Burgers, & Riemslag, 1992; Pangeni et al., 2010; Viswanathan, Frishman, & Robson, 2002).

For most stimulus conditions, the ERG phase changes of the F components were generally small (maximally 30°).

The time constants for amplitude and phase changes were between 1.9 and 5.7 min without any obvious differences in the changes for amplitudes or phases for the harmonic component or for the stimulus condition. Because the ERG measurements were performed with 2-min intervals, the estimated time constants suggest
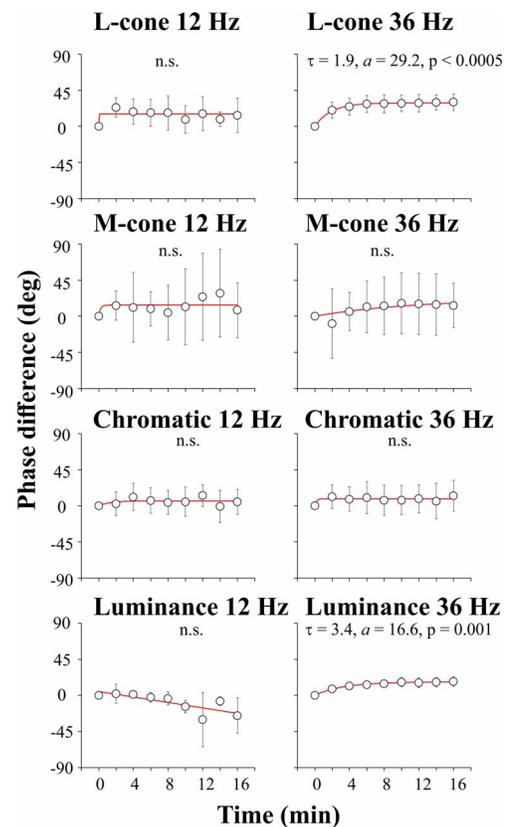
that the dynamics of adaptation are similar for the different stimulus conditions.

Changes in L/M ratios during adaptation

As mentioned above, the relative amplitude for the 36-Hz M-cone isolating stimulus increased more strongly than for the 36-Hz L-cone stimulus. This indicates that L/M ratios might change during adaptation. We, therefore, calculated the L/M ratios for all time points by dividing the L-cone–driven F amplitudes by the M-cone–driven F amplitudes at 12 and 36 Hz for each subject. Because ratios are not normally distributed, we calculated the logarithms of the individual ratios before averaging them and calculating them back into linear terms. The means ($\pm SD$) are shown as a function of adaptation time in Figure 6. In agreement with earlier data, the L/M ratios at 12 Hz were smaller than those at 36 Hz, consistent with the notion that the responses reflect luminance activity at 36 Hz and red–green chromatic activity at 12 Hz (Jacob et al., 2015; Kommanapalli, Murray, Kremers, Parry, & McKeefry, 2014; Kremers & Link, 2008; Kremers et al., 2010;
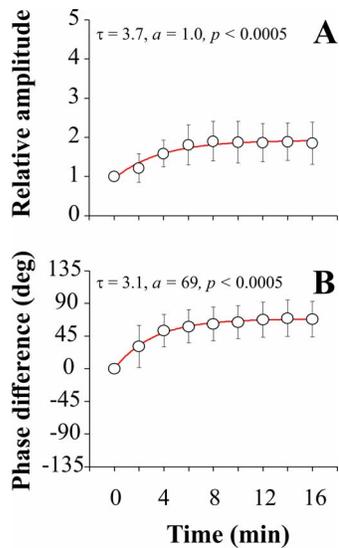
Brasil et al.

Figure 5. Averaged ($\pm$SD) normalized amplitude changes (A) and phase shifts (B) of the second harmonic component (2F) compared to the amplitude and phase at $t = 0$ as a function of adaptation time for the 12-Hz luminance stimulus. The data are presented in a similar manner as in Figure 3.

Martins et al., 2016). Interestingly, the L/M ratios did not change strongly during the course of light adaptation with 12-Hz stimuli, whereas they decreased with adaption time for the 36-Hz stimuli. Thus, luminance-reflecting responses are strongly L-cone dominated directly after onset of the adapting light. M-cone–driven responses increase more strongly over time, resulting in a decrease of the L/M ratio. It is unlikely that this reflects differences in physiological properties between the L- and M-cones because, in that case, the ratios with 12 Hz would be expected to have changed as well.

There were no indications of consistent changes in phase differences between L- and M-cone–driven ERGs with adaptation time (data not shown). In agreement with previous data (Jacob et al., 2015; Kremers & Pangeni, 2012), the phase differences between L- and M-cone–driven responses were about 180° (189° $\pm$ 36° average over all subjects and adaptation times) at 12 Hz consistent with L-M cone opponent processing. At 36 Hz, the phase differences were larger (224° $\pm$ 35° average over all subjects and adaptation times).

Discussion

The aim of the present study was to describe light-adaptation processes after extended dark-adaptation for ERG mechanisms that are driven by L- and M-cones and that reflect the activity of cone opponent and
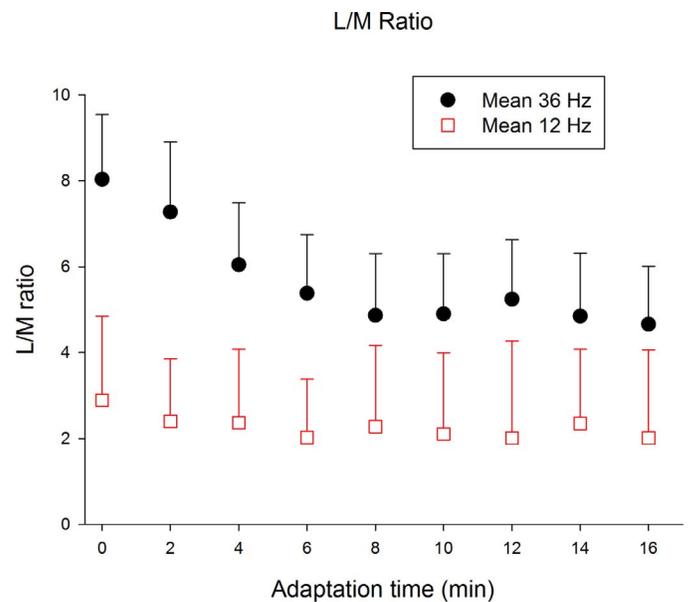

Figure 6. Mean L/M cone ERG amplitude ratio of the F components as a function of adaptation time obtained with 12- and 36-Hz L- and M-cone isolating stimuli. The ratios from 12-Hz data did not change during the adaptation period and did not differ strongly from unity, suggesting cone-opponent processing. The ratios obtained from the 36-Hz ERGs were larger, suggesting a luminance input. Interestingly, the ratios at 36-Hz decreased during light adaptation.

luminance postreceptoral pathways (Jacob et al., 2015; Kommanapalli et al., 2014; Kremers & Link, 2008; Kremers et al., 2010; Martins et al., 2016). This study extends the data already available in the literature in several ways. First, similar to the method of McAnany and Nolan (2014), sinusoidal stimuli around a mean luminance and chromaticity were used instead of flashes or trains of flashes. In these stimuli, frequency and mean state of adaptation could be varied independently. This offered the possibility to measure responses to chromatic and luminance stimuli. Second, with the exception of the responses to 12-Hz luminance stimuli, all responses to sinusoidal stimuli are dominated by the fundamental component. By extracting the F component (and the 2F component for 12-Hz luminance stimuli), the major changes in the responses were described. Finally, the stimuli provided the possibility to isolate responses in one cone type through the triple silent substitution technique. We were, thus, able to measure ERGs that were exclusively driven by the L- or the M-cones.

In many conditions, the responses changed although there were large interindividual differences in the magnitudes of changes. We found that the responses changed significantly when they reflected luminance activity (i.e., responses to 36-Hz luminance, L-cone isolating, and M-cone isolating stimuli as well as to 12-

Hz luminance stimuli; the latter is dominated by the 2F component). From this, we conclude that ERG adaptation to photopic mean luminances following complete dark adaptation is mainly present in the luminance pathway. ERGs mainly reflecting red–green chromatic activity did not change significantly although Figure 1 indicates that the changes may become significant when more subjects are included. This might indicate that the chromatic pathway does adapt but less strongly. However, the ERGs to L- and M-cone isolating stimuli are only biased toward chromatic signals but do not isolate them. Therefore, it cannot be excluded that small luminance signals may also be responsible for these changes. For those conditions, in which significant changes were found, the time constants were in the order of 2–6 min without obvious differences between stimulus conditions, indicating that the adaptation processes in the luminance system are uniform.

It was proposed that light adaptation may induce a slow release of the rod-induced suppression of cone-driven signals (Arden & Frumkes, 1986; Cameron & Lucas, 2009; Kondo et al., 1999). The time constants, therefore, would reflect those of this release. This may explain why only the luminance responses adapt in our experiments because, in the macaque retina, MC cells of the luminance pathway receive strong rod input, whereas rod inputs to PC cells are small or absent (Lee, Smith, Pokorny, & Kremers, 1997). Interestingly, we recently found in mice that cone-driven signals do change nearly instantaneously after a change in light level, whereas rod-driven signals may change in the course of minutes (Joachimsthaler & Kremers, submitted). These data support on the one hand the conclusion that the increases may be caused by a disinhibition of cones by rods. On the other hand, the fast changes in the mouse cone-driven ERGs are different from the data in human subjects and may reflect species differences.

The high L/M ratio for responses to 36-Hz stimuli directly after light onset with the subsequent decrease may point at differences between different retinal locations because the peripheral retina is strongly L-cone dominated (Hagstrom, Neitz, & Neitz, 1998, 2000) leading to a very high L/M ratio, whereas the L/M ratio in the central retina is substantially smaller (Jacob et al., 2015; Kuchenbecker, Sahay, Tait, Neitz, & Neitz, 2008). The 36-Hz L/M ratios of the present study may be explained when the responses are dominated by the retinal periphery directly after light onset with subsequent recruitment of the central retina. However, this proposal is at odds with the data of Kondo et al. (1999), who found that multifocal ERG response increases were mainly found in the retinal periphery after light adaptation.

In agreement with previous data (Pangeni et al., 2010) the ERG responses to 12-Hz luminance stimuli indicated that they were determined by two independent luminance-driven waves. Our data indicate that these waves have different adaptation dynamics. As a result, the F and 2F components changed differently with the 2F components dominating after 16 min of light adaptation. In contrast to the responses to other conditions that are driven by a single luminance or chromatic pathway, we propose that the responses to 12-Hz luminance stimuli contain two luminance-driven mechanisms. An alternative explanation for the small F component for responses to 12-Hz luminance stimuli, based on the assumption that on- and off-responses are in counterphase at this frequency and, thus, cancel each other out (Kondo & Sieving, 2001), can neither explain the large 2F component nor the different changes in F and 2F during light adaptation.

Conclusion

Light adaptation after an extended period in the dark resulted mainly in response amplitude increases mainly in ERGs that reflect activity of the luminance pathway. The responses to 12-Hz luminance stimuli may be driven by two independent luminance mechanisms with different adaptation dynamics.

Keywords: retinal pathways, light adaptation, cone-specific pathways, luminance pathways, chromatic pathways

Acknowledgments

Corresponding author: Jan Kremers.
Email: jan.kremers@uk-erlangen.de.
Address: Department of Ophthalmology, University Hospital Erlangen, Erlangen, Germany.

References

Alexander, K. R., Raghuram, A., & Rajagopalan, A. S. (2006). Cone phototransduction and growth of the ERG b-wave during light adaptation. *Vision*

Research, 46(22), 3941–3948, https://doi.org/10.1016/j.visres.2006.04.015.

Arden, G. B., & Frumkes, T. E. (1986). Stimulation of rods can increase cone flicker ERGs in man. *Vision Research*, 26(5), 711–721, https://doi.org/10.1016/0042-6989(86)90085-4.

Armington, J. C., & Biersdorf, W. R. (1958). Long-term light adaptation of the human electroretinogram. *Journal of Comparative and Physiological Psychology*, 51(1), 1–5, https://doi.org/10.1037/h0044572.

Benoit, J., & Lachapelle, P. (1995). Light adaptation of the human photopic oscillatory potentials: Influence of the length of the dark adaptation period. *Documenta Ophthalmologica*, 89(3), 267–276, https://doi.org/10.1007/BF01203380.

Burian, H. M. (1954). Electric responses of the human visual system. *Archive of Ophthalmology*, 51, 509–524.

Burkhardt, D. A., & Gottesman, J. (1987). Light adaptation and responses to contrast flashes in cones of the walleye retina. *Vision Research*, 27(9), 1409–1420, https://doi.org/10.1016/0042-6989(87)90151-9.

Burns, S. A., Elsner, A. E., & Kreitz, M. R. (1992). Analysis of nonlinearities in the flicker ERG. *Optometry and Vision Science*, 69(2), 95–105, https://doi.org/10.1097/00006324-199202000-00002.

Cameron, M. A., & Lucas, R. J. (2009). Influence of the rod photoresponse on light adaptation and circadian rhythmicity in the cone ERG. *Molecular Vision*, 15, 2209–2216. Retrieved from http://www.pubmedcentral.nih.gov/articlerender.fcgi?artid=2773742&tool=pmcentrez&rendertype=abstract.

Dowling, J. E., & Ripps, H. (1971). S-potentials in the skate retina. Intracellular recordings during light and dark adaptation. *The Journal of General Physiology*, 58(2), 163–189, https://doi.org/10.1085/jgp.58.2.163.

Estévez, O., & Spekreijse, H. (1982). The "silent substitution" method in visual research. *Vision Research*, 22(6), 681–691, https://doi.org/10.1016/0042-6989(82)90104-3.

Estévez, O., & Spekreuse, H. (1974). A spectral compensation method for determining the flicker characteristics of the human colour mechanisms. *Vision Research*, 14(9), 823–830, https://doi.org/10.1016/0042-6989(74)90147-3.

Gouras, P., & MacKay, C. J. (1989). Growth in amplitude of the human cone electroretinogram with light adaptation. *Investigative Ophthalmology and Visual Science*, 30(4), 625–630.

Hagstrom, S. A., Neitz, J., & Neitz, M. (1998). Variations in cone populations for red-green color vision examined by analysis of mRNA. *NeuroReport*, 9(9), 1963–1967, https://doi.org/10.1097/00001756-199806220-00009.

Hagstrom, S. A., Neitz, M., & Neitz, J. (2000). Cone pigment gene expression in individual photoreceptors and the chromatic topography of the retina. *Journal of the Optical Society America A*, 17(3), 527–537, https://doi.org/10.1364/JOSAA.17.000527.

Jacob, M. M., Pangeni, G., Gomes, B. D., Souza, G. S., Filho, M. D. S., Silveira, L. C. L., & Kremers, J. (2015). The spatial properties of L- and M-cone inputs to electroretinograms that reflect different types of post-receptoral processing. *PLoS One*, 10(3):e0121218, https://doi.org/10.1371/journal.pone.0121218.

Kommanapalli, D., Murray, I. J., Kremers, J., Parry, N. R. A., & McKeefry, D. J. (2014). Temporal characteristics of L- and M-cone isolating steady-state electroretinograms. *Journal of the Optical Society of America A*, 31(4), A113–A120, https://doi.org/10.1364/josaa.31.00a113.

Kondo, M., Miyake, Y., Piao, C. H., Tanikawa, A., Horiguchi, M., & Terasaki, H. (1999). Amplitude increase of the multifocal electroretinogram during light adaptation. *Investigative Ophthalmology and Visual Science*, 40(11), 2633–2637.

Kondo, M., & Sieving, P. A. (2001). Primate photopic sine-wave flicker ERG: Vector modeling analysis of component origins using glutamate analogs. *Investigative Ophthalmology and Visual Science*, 42(1), 305–312.

Kremers, J. (2003). The assessment of L- and M-cone specific electroretinographical signals in the normal and abnormal human retina. *Progress in Retinal and Eye Research*, 22, 579–605, https://doi.org/10.1016/S1350-9462(03)00049-1.

Kremers, J., & Link, B. (2008). Electroretinographic responses that may reflect activity of parvo- and magnocellular post-receptoral visual pathways. *Journal of Vision*, 8(15):11, 1–14, https://doi.org/10.1167/8.15.11. [PubMed] [Article]

Kremers, J., & Pangeni, G. (2012). Electroretinographic responses to photoreceptor specific sine wave modulation. *Journal of the Optical Society of America A*, 29(2), A306–A316, https://doi.org/10.1364/JOSAA.29.00A306.

Kremers, J., Rodrigues, A. R., de Lima Silveira, L. C., & da Silva Filho, M. (2010). Flicker ERGs

representing chromaticity and luminance signals. *Investigative Ophthalmology and Visual Science*, *51*(1), 577–587, https://doi.org/10.1167/iovs.09-3899.

Kuchenbecker, J. A., Sahay, M., Tait, D. M., Neitz, M., & Neitz, J. (2008). Topography of the long- to middle-wavelength sensitive cone ratio in the human retina assessed with a wide-field color multifocal electroretinogram. *Visual Neuroscience*, *25*, 301–306, https://doi.org/10.1017/S0952523808080474.

Lee, B. B., Smith, V. C., Pokorny, J., & Kremers, J. (1997). Rod imputs to macaque ganglion cells. *Vision Research*, *37*(20), 2813–2828, https://doi.org/10.1016/S0042-6989(97)00108-9.

Martins, C. M. G., Tsai, T., Barboni, M. T. S., da Costa, M. F., Nagy, B., Ventura, D. F., & Kremers, J. (2016). The influence of stimulus size on heterochromatic modulation electroretinograms. *Journal of Vision*, *16*(8):13, 1–11, https://doi.org/10.1167/16.8.13. [PubMed] [Article]

Matthews, H. R., Murphy, R. L., Fain, G. L., & Lamb, T. D. (1988, July 7). Photoreceptor light adaptation is mediated by cytoplasmic calcium concentration. *Nature*, *334*(6177), 67–69, https://doi.org/10.1038/334067a0.

McAnany, J. J., & Nolan, P. R. (2014). Changes in the harmonic components of the flicker electroretinogram during light adaptation. *Documenta Ophthalmologica*, *129*(1), 1–8, https://doi.org/10.1007/s10633-014-9437-y.

McCulloch, D. L., Marmor, M. F., Brigell, M. G., Hamilton, R., Holder, G. E., Tzekov, R., & Bach, M. (2015). ISCEV standard for full-field clinical electroretinography (2015 update). *Documenta Ophthalmologica. Advances in Ophthalmology*, *130*(1), 1–12, https://doi.org/10.1007/s10633-014-9473-7.

Meigen, T., & Bach, M. (1999). On the statistical significance of electrophysiological steady-state responses. *Documenta Ophthalmologica*, *98*(3), 207–232, https://doi.org/10.1023/A:1002097208337.

Miller, S., & Sandberg, M. A. (1991). Cone electroretinographic change during light adaptation in retinitis pigmentosa. *Investigative Ophthalmology and Visual Science*, *32*(9), 2536–2541.

Miyake, Y., Horiguchi, M., Ota, I., & Shiroyama, N. (1987). Characteristic ERG-flicker anomaly in incomplete congenital stationary night blindness. *Investigative Ophthalmology & Visual Science*, *28*(11), 1816–1823.

Murayama, K., & Sieving, P. A. (1992). Different rates of growth of monkey and human photopic a-, b-, and d-waves suggest two sites of ERG light adaptation. *Clinical Vision Sciences*, *7*(5), 385–392.

Normann, R. A., & Perlman, I. (1979). The effects of background illumination on the photoresponses of red and green cones. *The Journal of Physiology*, *286*(1), 491–507, https://doi.org/10.1113/jphysiol.1979.sp012633.

Odom, J. V., Reits, D., Burgers, N., & Riemslag, F. C. C. (1992). Flicker electroretinograms: A systems analytic approach. *Optometry and Vision Science*, *69*(2), 106–116, https://doi.org/10.1097/00006324-199202000-00003.

Pangeni, G., Horn, F. K., & Kremers, J. (2010). A new interpretation of components in the ERG signals to sine wave luminance stimuli at different temporal frequencies and contrasts. *Visual Neuroscience*, *27*(3–4), 79–90, https://doi.org/10.1017/S0952523810000179.

Parry, N. R. A., Murray, I. J., Panorgias, A., Mckeefry, D. J., Lee, B. B., & Kremers, J. (2012). Simultaneous chromatic and luminance human electroretinogram responses. *Journal of Physiology*, *590*(13), 3141–3154, https://doi.org/10.1113/jphysiol.2011.226951.

Peachey, N. S., Alexander, K. R., Derlacki, D. J., & Fishman, G. A. (1992). Light adaptation, rods, and the human cone flicker ERG. *Visual Neuroscience*, *8*(2), 145–150, https://doi.org/10.1017/S0952523800009305.

Peachey, N. S., Alexander, K. R., & Fishman, G. A. (1991). Visual adaptation and the cone flicker electroretinogram. *Investigative Ophthalmology and Visual Science*, *32*(5), 1517–1522.

Peachey, N. S., Alexander, K. R., Fishman, G. A., & Derlacki, D. J. (1989). Properties of the human cone system electroretinogram during light adaptation. *Applied Optics*, *28*(6), 1145–1150, https://doi.org/10.1364/AO.28.001145.

Shapiro, A. G., Pokorny, J., & Smith, V. C. (1996). Cone-rod receptor spaces with illustrations that use CRT phosphor and light-emitting-diode spectra. *Journal of the Optical Society of America A, Optics, Image Science, and Vision*, *13*(12), 2319–2328, https://doi.org/10.1364/JOSAA.13.002319.

Viswanathan, S., Frishman, L. J., & Robson, J. G. (2002). Inner-retinal contributions to the photopic sinusoidal flicker electroretinogram of macaques: Macaque photopic sinusoidal flicker ERG. *Documenta Ophthalmologica*, *105*(2), 223–242, https://doi.org/10.1023/A:1020505104334.